layers, owing to the charge imbalance, which is in agreement with recent experiments[22,23]. This is because the suppression of the superconducting order parameter in the inner layers will enhance the pseudogap. The single-particle excitation spectra as observed in angle-resolved photoemission spectroscopy (ARPES) of multilayer copper oxides should be sensitive to the doping imbalance of the layers; there is already some indication of this in experiments[26,27] involving the triple-layer material Bi2223. Although bilayer splitting is observed in optimally doped Bi2212, trilayer and higher-multilayer splittings will be increasingly difficult to observe, because of the induced pseudogap of the inner layers.

We also predict that the maximum superconducting gap measured in ARPES will be a bell-shaped curve as a function of n with a maximum at $n = 3$. It would be worth investigating whether the recently developed Fourier-transform scanning tunnelling spectroscopy (FT-STS)[28] could provide layer-specific information. The change in the spectra with increasing n should be detectable, as the tunnelling rate falls off exponentially with the distance. For this, it would be interesting to consider an underdoped sample. As n increases, the spectra, which would be dominated by the outer layer, will change because of its increased doping. □

Received 16 November 2003; accepted 16 January 2004; doi:10.1038/nature02348.

1. Scott, B. A. *et al.* Layer dependence of the superconducting transition temperature of $HgBa_2Ca_{n-1}Cu_nO_{2n+2+\delta}$. *Physica C* **230,** 239–245 (1994).
2. Chakravarty, S., Sudbø, A., Anderson, P. W. & Strong, S. Interlayer tunneling and gap anisotropy in high-temperature superconductors. *Science* **261,** 337–340 (1993).
3. Kotegawa, H. *et al.* NMR study of carrier distribution and superconductivity in multilayered high-T_c cuprates. *J. Phys. Chem. Solids* **62,** 171–175 (2001).
4. Perali, A., Castellani, S., Di Castro, C. & Grilli, M. *d*-wave superconductivity near charge instabilities. *Phys. Rev. B* **54,** 16216–16225 (1996).
5. Tallon, J. L. *et al.* Critical doping in overdoped high-T_c superconductors: a quantum critical point? *Phys. Status Solidi B* **215,** 531–540 (1999).
6. Kivelson, S. A., Fradkin, E. & Emery, V. J. Electronic liquid-crystal phases of a doped Mott insulator. *Nature* **393,** 550–553 (1998).
7. Varma, C. M. Pseudogap phase and the quantum-critical point in copper-oxide metals. *Phys. Rev. Lett.* **83,** 3538–3541 (1999).
8. Chakravarty, S., Laughlin, R. B., Morr, D. K. & Nayak, C. Hidden order in the cuprates. *Phys. Rev. B* **63,** 094503 (2001).
9. Sachdev, S. Colloquium: Order and quantum phase transitions in the cuprate superconductors. *Rev. Mod. Phys.* **75,** 913–932 (2003).
10. Balakirev, F. F. *et al.* Signature of optimal doping in Hall-effect measurements on a high-temperature superconductor. *Nature* **424,** 912–915 (2003).
11. Jansen, L. & Block, R. On the relation between (maximum) critical temperature and *c*-axis layered structure in cuprates. I. Evaluation of existing analyses. *Physica A* **289,** 165–177 (2001).
12. Anderson, P. W. *c*-axis electrodynamics as evidence for the interlayer theory of high-temperature superconductivity. *Science* **279,** 1196–1198 (1998).
13. Moler, K. A., Kirtley, J. R., Hinks, D. G., Li, T. W. & Ming, X. Images of interlayer Josephson vortices in $Tl_2Ba_2CuO_{6+\delta}$. *Science* **279,** 1193–1196 (1998).
14. Chakravarty, S., Kee, H.-Y. & Abrahams, E. Frustrated kinetic energy, the optical sum rule, and the mechanism of superconductivity. *Phys. Rev. Lett.* **82,** 2366–2369 (1999).
15. Boris, A. V. *et al.* Josephson plasma resonance and phonon anomalies in trilayer $Bi_2Sr_2Ca_2Cu_3O_{10}$. *Phys. Rev. Lett.* **89,** 277001 (2002).
16. Timusk, T. & Statt, B. The pseudogap in high-temperature superconductors: an experimental survey. *Rep. Prog. Phys.* **62,** 61–122 (1999).
17. Khlebnikov, S. Interlayer tunnelling in a non-Fermi-liquid metal. *Phys. Rev. B* **53,** R11964–R11967 (1996).
18. Arrigoni, E., Fradkin E. & Kivelson S. A. Mechanism of high temperature superconductivity in a striped Hubbard model. Preprint at ⟨http://arXiv.org/abs/cond-mat/0309572⟩ (2003).
19. Chakravarty, S. Do electrons change their *c*-axis kinetic energy upon entering the superconducting state? *Eur. Phys. J. B* **5,** 337–343 (1998).
20. Bozovic, I. *et al.* No mixing of superconductivity and antiferromagnetism in a high-temperature superconductor. *Nature* **422,** 873–875 (2003).
21. Chakravarty, S., Kee, H.-Y. & Nayak, C. Neutron scattering signature of *d*-density wave order in the cuprates. *Int. J. Mod. Phys. B* **15,** 2901–2909 (2001).
22. Tokunaga, Y. *et al.* Effect of carrier distribution on superconducting characteristics of the multilayered high-T_c cuprate $(Cu_{0.6}C_{0.4})Ba_2Ca_3CuO_{12+y}$: Cu-63-NMR study. *Phys. Rev. B* **61,** 9707–9710 (2000).
23. Kotegawa, H. *et al.* Unusual magnetic and superconducting characteristics in multilayered high-T_c cuprates: ^{63}Cu1 NMR study. *Phys. Rev. B* **64,** 064515 (2001).
24. Emery, V. J. & Kivelson, S. A. Importance of phase fluctuations in superconductors with small superfluid density. *Nature* **374,** 434–437 (1995).
25. Carlson, E. W., Kivelson, S. A., Emery, V. J. & Manousakis, E. Classical phase fluctuations in high temperature superconductors. *Phys. Rev. Lett.* **83,** 612–615 (1999).
26. Feng, D. L. *et al.* Electronic structure of the trilayer cuprate superconductor $Bi_2Sr_2Ca_2Cu_3O_{10+\delta}$. *Phys. Rev. Lett.* **88,** 107001 (2002).
27. Sato, T. *et al.* Low energy excitation and scaling in $Bi_2Sr_2Ca_{n-1}Cu_nO_{2n+4}$ (n = 1 − 3): angle-resolved photoemission spectroscopy. *Phys. Rev. Lett.* **89,** 067005 (2002).
28. McElroy, K. *et al.* Relating atomic-scale electronic phenomena to wave-like quasiparticle states in superconducting $Bi_2Sr_2CaCu_2O_{8+\delta}$. *Nature* **422,** 592–596 (2003).
29. Yamauchi, H., Karppinen, M. & Tanaka, S. Homologous series of layered cuprates. *Physica C* **263,** 146–150 (1996).
30. Kuzemskaya, I. G., Kuzemsky, A. L. & Cheglokov, A. A. Superconducting properties of the family of mercurocuprates and role of layered structure. *J. Low-Temp. Phys.* **118,** 147–152 (2000).

Acknowledgements We thank the Aspen Centre for Physics, where this collaboration was initiated, and also N. P. Armitage and J. Hoffman for discussions. We acknowledge support from the US National Science Foundation (S.C.), the Canadian Institute for Advanced Research (H.-Y.K. and K.V.), and the Alfred P. Sloan Foundation (H.-Y.K.).

Competing interests statement The authors declare that they have no competing financial interests.

Correspondence and requests for materials should be addressed to S.C. (sudip@physics.ucla.edu).

Crystal symmetry and the reversibility of martensitic transformations

Kaushik Bhattacharya[1], Sergio Conti[2], Giovanni Zanzotto[3] & Johannes Zimmer[2]

[1]*Division of Engineering and Applied Science, California Institute of Technology, Pasadena, California 91125, USA*
[2]*Max Planck Institute for Mathematics in the Sciences, Inselstrasse 22, 04103 Leipzig, Germany*
[3]*Dipartimento di Metodi e Modelli Matematici per le Scienze Applicate, Università di Padova, Via Belzoni 7, 35131 Padova, Italy*

Martensitic transformations are diffusionless, solid-to-solid phase transitions, and have been observed in metals, alloys, ceramics and proteins[1,2]. They are characterized by a rapid change of crystal structure, accompanied by the development of a rich microstructure. Martensitic transformations can be irreversible, as seen in steels upon quenching[1], or they can be reversible, such as those observed in shape-memory alloys[3,4]. In the latter case, the microstructures formed on cooling are easily manipulated by loads and disappear upon reheating. Here, using mathematical theory and numerical simulation, we explain these sharp differences in behaviour on the basis of the change in crystal symmetry during the transition. We find that a necessary condition for reversibility is that the symmetry groups of the parent and product phases be included in a common finite symmetry group. In these cases, the energy barrier to lattice-invariant shear is generically higher than that pertaining to the phase change and, consequently, transformations of this type can occur with virtually no plasticity. Irreversibility is inevitable in all other martensitic transformations, where the energy barrier to plastic deformation (via lattice-invariant shears, as in twinning or slip) is no higher than the barrier to the phase change itself. Various experimental observations confirm the importance of the symmetry of the stable states in determining the macroscopic reversibility of martensitic transformations.

Martensitic transformations have numerous technological applications, particularly in steel, where the transformation induced by quenching (fast cooling) is exploited for enhancing the alloy's strength[1]. Another application is the fascinating shape-memory effect in alloys like Nitinol, used in medical and engineering devices[3]. Martensitic phase changes are also exploited to toughen structural ceramics[5] such as zirconia, and are observed in biological systems such as the tail sheath of the T4 bacteriophage virus[6]. The study of these transformations has led to improved materials for actuation (ferromagnetic shape-memory alloys[7,8] and ferroelectrics[9]) and to candidates for artificial muscles[10]. Finally, the rich

microstructure (distinctive patterns developed at scales ranging from a few nanometres to a few micrometres) that accompanies these transformations provides a valuable test case for the development of multi-scale modelling tools[11].

In some materials, such as shape-memory alloys, the martensitic phase change is almost perfectly reversible (often termed 'thermoelastic')[3,4]. When cooling a shape-memory alloy like Nitinol from high temperature, the transformation produces a microstructure with a (twinned) plate-like morphology. This microstructure can easily be changed by the application of loads. The transformation can be completely reversed, with the disappearance of the microstructure upon reheating and the appearance of little or no dislocation or twinning in the parent (high temperature, high symmetry) phase.

In contrast, the martensitic transformation is not reversible in materials like steel and other alloys, such as CoNi[1]. In steels, the microstructure forms in a sudden burst with a lath-like morphology upon cooling, and is immobile on loading. Moreover, the transformation is irreversible and the microstructure does not disappear upon reheating. In CoNi the phase change is also irreversible, as successive microstructures form both on heating and cooling. Materials that undergo irreversible transformations are characterized by significant dislocations and twinning in the parent phase.

We provide an explanation for this difference in reversibility on the basis of the symmetry change during the transformation. We label as 'weak' the martensitic transformations in which the symmetry group of both the parent and product phase are included in a common finite symmetry group[12] (which includes symmetry breaking), and all others as 'reconstructive'[13] (note that this is different from the usage of the term 'reconstructive' to mean 'diffusional': all the transformations considered here are diffusionless). We show through rigorous mathematical theory and numerical simulation that irreversibility is inevitable in a reconstructive phase transformation, but not in a weak one.

Figure 1 illustrates our main idea through a square-to-hexagonal reconstructive phase change in a two-dimensional crystal. Consider the square lattice shown on the left, and suppose the solid square unit cell is transformed to the solid unit cell of the hexagonal lattice (middle). By symmetry the solid and dashed unit cells shown in the middle are equivalent. If the crystal is transformed back to the square phase, the dashed hexagonal cell can go to, say, the dashed cell on the right. Crucially, the square cell on the left is then transformed to the sheared cell of the square lattice on the right. Thus, upon transforming, performing a symmetry operation, and transforming back, the crystal has undergone a lattice-invariant shear, that is, a shearing deformation that leaves the entire (ideal, infinite) lattice invariant. This also holds for finite lattices if boundary effects can be neglected, as illustrated below by means of numerical simulations, showing dislocations and plastic deformation.

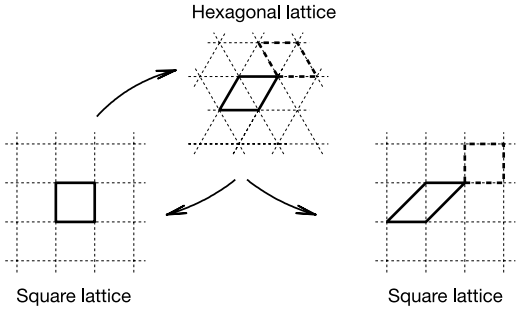

Figure 1 A lattice-invariant shear can be generated by a forward and reverse square-to-hexagonal phase transformation. The transformation takes the solid square on the left to the solid rhombus in the middle. The hexagonal symmetry implies the equivalence of the solid rhombic cell to the dashed rhombic one. The reverse transformation takes the latter to the dashed square on the right. In the process, the original solid square on the left has sheared by a lattice-invariant shear to the solid parallelogram on the right.

Various experimental observations confirm our predictions. Pure iron (Fe) undergoes a temperature-induced reconstructive γ–α (face-centred-cubic to body-centred-cubic, f.c.c.-to-b.c.c.) transformation. As Ni and C are added to obtain steel, the martensite becomes body-centred-tetragonal (b.c.t.) with an increasing tetragonality, so that the martensitic transformation becomes weak. Correspondingly, Maki and Tamura[14] found that with increasing Ni and C the reversibility of the phase changes increased, the amount of plastic deformation decreased, and the morphology changed from lath to butterfly to lenticular to plate-like. Iron also undergoes a pressure-induced reconstructive α–ϵ (b.c.c. to hexagonal-close-packed, h.c.p.) transformation, again accompanied by twins and dislocations[15,16]. Another set of observations concern materials undergoing the reconstructive f.c.c.-to-h.c.p. transformation. Liu *et al.*[17] considered the CoNi system; they hardened the parent phase to prevent any plastic deformation, but found that the transformation was still irreversible, with both heating and cooling producing twins and plastic deformation. Similar observations were made in FeMnCrSiNi steels[18,19]. Finally, in a block co-polymer, the (reconstructive) b.c.c.-to-hexagonal transformation was observed to be irreversible because of orientation proliferation through twinning in both phases[20].

In spirit, our results are related to those of Otsuka and Shimizu[21], who discuss the effects of ordering on crystallographic reversibility of martensitic transformation in alloys. They[21] observe that in ordered alloys the transformation path must be such that the order is not destroyed, whereas in disordered ones only the atomic positions need to be recovered. Their results are consistent with many experiments, but they also note that the f.c.c.-to-face-centred-tetragonal (f.c.t.) transformation is an 'exception', which, they argue, is a consequence of the fact that "the lattice correspondence is unique in the reverse transformation because of the so simple lattice change and lower symmetry of the f.c.t. phase". We show here that the essential difference resides in the crystal symmetry, rather than in order and disorder. This provides a general framework which includes both their[21] theory and exception, and also extends to other situations.

The common explanation (in ref. 14, for example) for the irreversibility in Fe (or low-Ni or -C steels) is based on the volume change that accompanies the transformation. The idea is that a partially transformed region causes stress and plastic deformation. However, a system like the styrene block co-polymer of ref. 20 should be largely unaffected by any volume change. Our explanation is independent of such a volume effect. It is possible, however, that both mechanisms contribute to the irreversibility in Fe.

As our result is based only on the symmetry of the energetic landscape, it is independent of material parameters, such as elastic moduli. We show that the barrier to lattice-invariant shears in reconstructive transformations is as high as to the phase transition itself. A remarkable implication is that reconstructive transformations are accompanied by plastic deformation through dislocations and twinning in the parent phase, making these phase changes irreversible. In contrast, weak transformations have the potential to be reversible, because the energy barriers to lattice-invariant shears and to the phase transition are independent of each other. Our numerical simulations indicate that weak transformations are indeed generically reversible. Yet the two energy barriers might happen to be comparable in particular materials undergoing a weak transformation. This, for example, is the case in Ni–50Ti, where plastic deformation masks the reversibility. However, (precipitate) hardening this material makes these barriers different, thereby revealing the reversible character of the underlying weak

transformation[3]. In contrast, hardening does not rescue the irreversibility of CoNi[17] or FeMnCrSiNi[18,19], which undergo reconstructive transformations. In summary, a transformation must be weak to be reversible.

Another consequence of our remarks is that materials like FeNi should be comparatively softer at compositions that are closer to a reconstructive transformation. This effect, however, may be obscured by the fact that the very softness of the ideal lattice produces plastic deformation and the entanglement of dislocations in the crystal, leading eventually to hardening. None of these phenomena are present in crystals undergoing weak martensitic transformations.

We now present the general theory followed by a concrete example, and numerical simulations. We state the theory for the simple case of Bravais lattices, which can readily be extended to crystals whose translational symmetry is continuous across the phase change. A Bravais lattice $\mathcal{L}(\boldsymbol{e}_i)$ is given by the linear combinations, with integral coefficients, of three independent vectors $\{e_1, e_2, e_3\}$ forming the lattice basis. Another basis $\{f_1, f_2, f_3\}$ generates the same lattice, $\mathcal{L}(\boldsymbol{e}_i) = \mathcal{L}(\boldsymbol{f}_i)$, if and only if $\boldsymbol{f}_i = \sum_{j=1}^{3} m_i^j \boldsymbol{e}_j$ with a matrix m belonging to the group[12,22,23]:

$$\mathcal{G} := \{m : m_i^j \text{ integers and } \det(m) = \pm 1\} \quad (1)$$

which is the global symmetry group of Bravais lattices. Applied to any given lattice, $\mathcal{G}$ consists of rotations, reflections, lattice-invariant shears and combinations thereof; the restriction to rotations and reflections gives the lattice group (a matrix representation of the point group) of that lattice.

The free-energy density Φ of the crystal is a function of the lattice basis at a fixed temperature. It is invariant under the global symmetry group $\mathcal{G}$, as it cannot distinguish among bases generating the same lattice[11,23,24]:

$$\Phi(\boldsymbol{e}_i) = \Phi(m_i^j \boldsymbol{e}_j) \text{ for every } m \in \mathcal{G} \quad (2)$$

This global framework takes all possible deformations into account, including large shearing distortions. From equation (2), the energy landscape of the crystal has infinitely many wells, which are not contained in any bounded region in strain space (see Fig. 2).

For weak martensitic transformations the invariance of the energy (equation (2)) can be limited to a finite subgroup of $\mathcal{G}$ owing to the group–subgroup relation; correspondingly, the domain of the energy can be restricted to a neighbourhood of the reference configuration. This neighbourhood does not contain any lattice-invariant shears and only contains a finite number of energy wells. Such domains are called Ericksen–Pitteri neighbourhoods (EPNs)[24,25]; see Fig. 2. Therefore, the classical framework of Landau theory and nonlinear elasticity[11,23,26] applies in these cases.

For reconstructive martensitic transformations, on the other hand, the symmetry decreases along the transformation path, but increases again at the final state, and there is no reference configuration whose lattice group contains those of the two given phases.

We establish the following mathematical fact: the lattice groups of the two phases in any reconstructive transformation necessarily generate unbounded shear-like distortions. Consequently, the barrier between the infinitely many energy wells of the crystal is, at most, equal to that of the underlying phase change. This implies that the material cannot resist certain arbitrarily large deformations, which makes the reconstructive transformation necessarily non-thermoelastic and irreversible, owing to the creation of defects in the lattice. At the same time, no reduction to a finite number of wells in a bounded region is possible (no EPN can be extracted) and the classical approach of the Landau type is not applicable. (Some authors have extended the Landau framework to encompass reconstructive transformations by introducing a "transcendental order parameter"[13], which gives a partial description of the lattice periodicity characterized by the global group $\mathcal{G}$.)

We show in the Methods section that in a reconstructive transformation an unbounded element of $\mathcal{G}$ is always generated. Precisely, we necessarily obtain an element with an infinite period (that is whose powers can become arbitrarily large), akin to slip and twinning in the parent phase. We note further that the most common reconstructive transformations involve phases with maximal point symmetry: the primitive-cubic, the f.c.c., the b.c.c., or the hexagonal subgroups of $\mathcal{G}$. For instance, consider an f.c.c. lattice. For some transformations to b.c.c., such as the Bain stretch considered below, the symmetry groups of the two lattices generate the entire group $\mathcal{G}$, with its full set of lattice-invariant shears. The same happens for any transformation between phases with maximal symmetry.

The impossibility of restricting the symmetry to a finite subgroup of $\mathcal{G}$, and the energy domain to a suitable EPN, has dramatic implications for the variational treatment of reconstructive phase transformations. Indeed, if we assume that the deformation at each time is determined by minimizing the free-energy subject to external forces and boundary conditions, the invariance of the energy under the whole group $\mathcal{G}$ implies that the solid cannot resist any shear[27]. In practice, dynamics and defects, including dislocations, moderate this phenomenon, which we revisit through our numerical simulations.

We now focus on a concrete case study, demonstrating that the

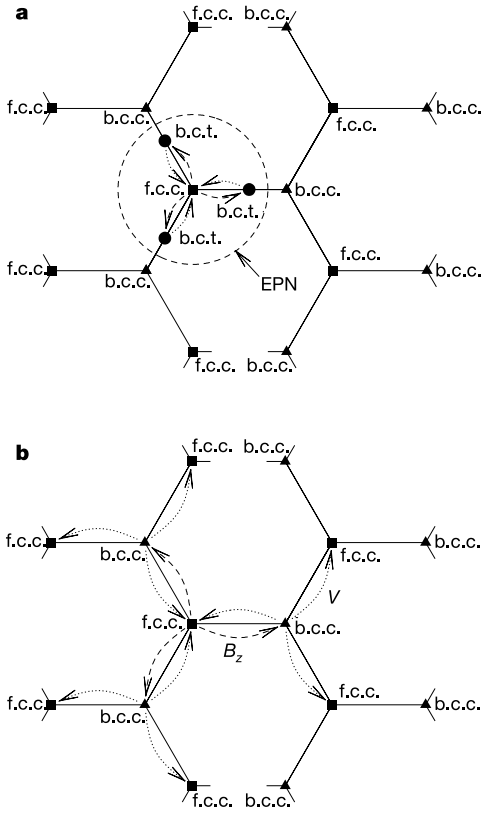

Figure 2 Schematic representation of weak versus reconstructive transformations in the space of lattices. **a**, Weak. A uniaxial deformation (dashed arrows) of the f.c.c. lattice (represented by squares) can give three equivalent b.c.t. lattices (circles). The reverse transformation (dotted arrows) returns to the original f.c.c. configuration. All the transformation strains are confined within a single EPN, such as the dashed circle. **b**, Reconstructive f.c.c.-to-b.c.c.. The transformation B_z leads from an f.c.c. lattice to three equivalent b.c.c. lattices, and the reverse transformation (such as V) from each b.c.c. lattice can proceed to three distinct but equivalent f.c.c. lattices, and so on. No EPN can be singled out.

composition of an f.c.c.-to-b.c.c. (forward) transformation and a b.c.c.-to-f.c.c. (reverse) transformation can in fact result in a lattice-invariant shear. We start from an f.c.c. lattice aligned with the coordinate axes, and subject it to a uniaxial stretch U_z along the z axis:

$$U_z^{(\lambda)} = \begin{pmatrix} 1 & 0 & 0 \\ 0 & 1 & 0 \\ 0 & 0 & 1/\lambda \end{pmatrix},$$

neglecting volumetric changes. For λ between 1 and $\sqrt{2}$, the product lattice has tetragonal symmetry, and we have a weak transformation. When λ is equal to $\sqrt{2}$, we obtain the Bain stretch $U_z^{(\sqrt{2})} = B_z$ which produces the b.c.c. lattice in a reconstructive transformation: see Fig. 3. Now consider the reverse b.c.c.-to-f.c.c. transformation: it can occur in three possible ways, owing to the symmetry of the b.c.c. phase. A crucial point is that the four-fold symmetry axes of the b.c.c. lattice are different from those of the initial f.c.c. crystal. One of the three possibilities for the reverse stretch corresponds to B_z^{-1}, and leads back to the original lattice. The other two are stretches along the $(1,\pm1, 0)$ directions (still using the original coordinate system). For instance, let us consider the reverse stretch V along the $(1, 1, 0)_{\text{f.c.c.}}$ direction, which can be expressed as

$$V = QB_z^{-1}Q^T$$

where Q is the 90-degree rotation with axis $(1, -1, 0)$, which belongs to the point group of the b.c.c. phase. After applying V, the final lattice is again f.c.c.; however, the total transformation gives:

$$VB_z = QB_z^{-1}Q^TB_z = RS$$

where R is a rotation and S is a shear on a $\{111\}_{\text{f.c.c.}}$ plane along a $\langle 112\rangle_{\text{f.c.c.}}$ direction. We can check that S brings the original f.c.c. basis to a $\mathcal{G}$-equivalent one, that is, the transformation VB_z restores the f.c.c. lattice to itself up to the inessential rigid-body rotation R (see Fig. 3). Successive iterations of VB_z then generate larger and larger lattice-invariant deformations, and similar strategies can generate the entire group $\mathcal{G}$. The barrier between the $\mathcal{G}$-related sheared configurations originated in this way is exactly equal to the barrier pertaining to the phase transformation. If only part of the crystal undergoes the VB_z transformation, while the rest goes back to the original state, a Shockley partial dislocation with Burgers vector $\frac{1}{6}\langle 112\rangle$ is formed[28]. The double transformation $(VB_z)^2$ then gives the Burgers vector $\frac{1}{2}\langle 110\rangle$. Both kinds are typical of f.c.c. crystals. When starting from a b.c.c. crystal, this same mechanism generates dislocations with Burgers vector $\langle 111\rangle_{\text{b.c.c.}}$ on $\{112\}_{\text{b.c.c.}}$ planes, which are among the most common ones in b.c.c. lattices.

We also illustrate the phenomena that are discussed above for finite domains in the presence of boundary conditions, with numerical simulations done for simplicity for a square-to-hexagonal transformation in two dimensions. We consider a 50×50 grid of atoms interacting with a three-body nearest-neighbour potential[29], which produces for the crystal a two-dimensional version of the $\mathcal{G}$-invariant energy in equation (2).

The simulation of a shearing experiment of a crystal close to a reconstructive phase transformation is shown in Fig. 4b. As the left and the right boundaries are progressively displaced, dislocations form in the lattice, which lead to irreversible plastic deformations and defects in the crystal.

In contrast, Fig. 4d shows the same simulation for a crystal close to a square-to-rhombic symmetry-breaking (weak) transformation. In this case, no dislocations arise in the lattice. Instead, typical layered martensitic twins mixing with the higher-symmetry parent

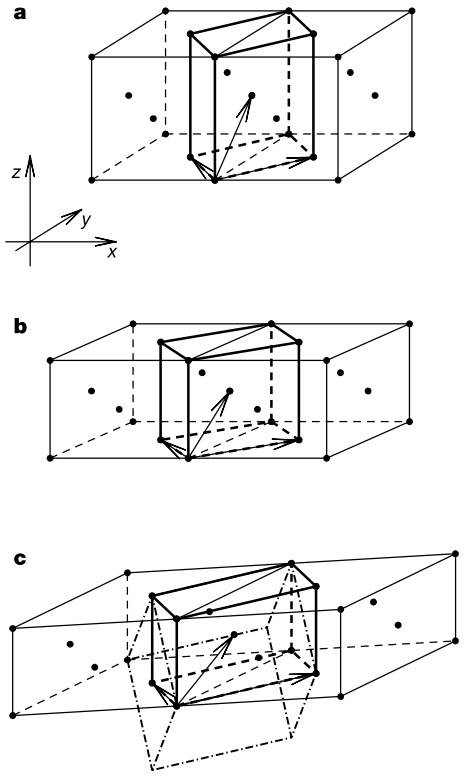

Figure 3 Shear generated for an f.c.c.-to-b.c.c. transformation in an f.c.c.–b.c.c.–f.c.c. cycle. **a**, An f.c.c. lattice, with a b.c.t. cell highlighted. **b**, The uniaxial Bain stretch B_z transforms the b.c.t. cell to the b.c.c. one. **c**, The inverse Bain stretch $V = QB_z^{-1}Q^T$ transforms the crystal back to f.c.c. (dash-dotted bold f.c.c. cell highlighted), but sheared relative to the original. The arrows show a basis undergoing the lattice-invariant shear.

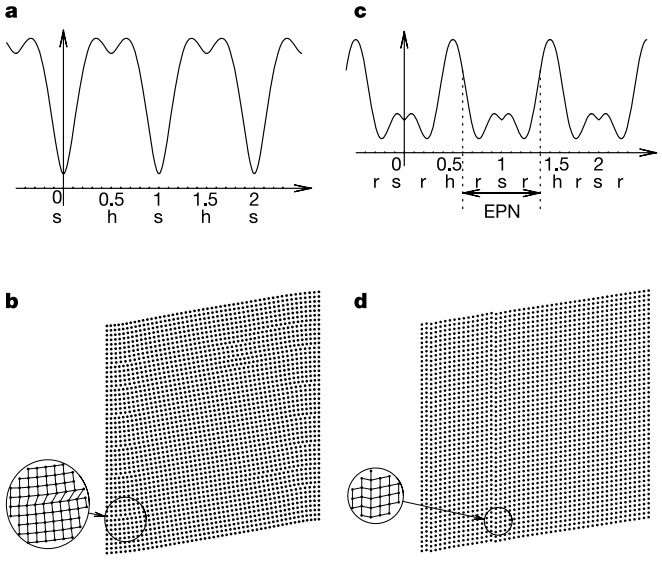

Figure 4 Reconstructive transformations generate dislocations, weak ones do not. **a**, **b**, Reconstructive transformation. **c**, **d**, Weak transformation. **a**, Section of the energy profile of a crystal close to a square-to-hexagonal (s–h) transformation, along a s–h–s line. The energy has the full invariance (2), with minima s and h plotted respectively at positions 0, 1, and 0.5, 1.5, and so on. **b**, An incremental shear test with boundary conditions on the left and right side results in dislocations. **c**, Section of the generic energy profile of a crystal close to a square-to-rhombic (s–r) transformation, along a s–r–h line. The square states s in 0, 1, and so on are metastable, and additional minima are present at intermediate rhombic configurations r, with hexagonal maxima at 0.5, 1.5, and so on. **d**, The same incremental shear test results in no dislocations, but only reversible transformation twins, because starting from the square minimum at 0, the 'faraway' square at 1 is not reachable by overcoming a small energy barrier.

phase can be observed, which accommodate the imposed boundary condition in a reversible way (this is the origin of the memory effect). □

Methods

To prove that in a reconstructive transformation an aperiodic element of $\mathcal{G}$ (called GL(3, $\mathbb{Z}$) in algebra) is generated, we first note that any lattice group is finite, and conversely any finite subgroup of $\mathcal{G}$ is included in the lattice group of some lattice (see proposition 3.5 in ref. 23). Thus a transformation is weak if and only if the lattice groups of the two crystal phases generate a finite group. Therefore a reconstructive transformation produces an infinite subgroup of $\mathcal{G}$ with a finite number of generators. Such a group necessarily contains an element with no finite period as a consequence of the Burnside–Schur theorem on periodic groups.

We finally establish that for any pair of Bravais lattices with maximal point symmetry there are reconstructive transformations that generate the entire group $\mathcal{G}$. Indeed, it is readily verified that for suitable pairs of subgroups in $\mathcal{G}$ belonging to the four arithmetic classes with maximal point symmetry one can produce all the generators of $\mathcal{G}$, that is, a suitable reflection, permutation and simple shear[30].

Received 2 September 2003; accepted 28 January 2004; doi:10.1038/nature02378.

1. Olson, G. B. & Owen, W. (eds) *Martensite* (ASM International, Materials Park, OH, 1992).
2. Salje, E. K. H. *Phase Transitions in Ferroelastic and Co-elastic Crystals* (Cambridge Univ. Press, Cambridge, 1993).
3. Otsuka, K. & Wayman, C. M. *Shape Memory Materials* (Cambridge Univ. Press, Cambridge, 1998).
4. Barrett, C. S. & Massalski, T. B. *Structure of Metals* 3rd edn (Pergamon, Oxford, 1987).
5. Bocanegra-Bernal, M. H. & De la Torre, S. D. Phase transitions in zirconium dioxide and related materials for high performance engineering ceramics. *J. Mater. Sci.* **37,** 4947–4971 (2002).
6. Olson, G. B. & Hartman, H. Martensite and life—displacive transformations as biological processes. *J. Physique* **43**(C4), 855–865 (1982).
7. James, R. D. & Wuttig, M. Magnetostriction of martensite. *Phil. Mag. A* **77,** 1273–1299 (1998).
8. Sozinov, A., Likhachev, A. A., Lanska, N. & Ullakko, K. Giant magnetic-field-induced strain in NiMnGa seven-layered martensitic phase. *Appl. Phys. Lett.* **80,** 1746–1748 (2002).
9. Shu, Y. C. & Bhattacharya, K. Domain patterns and macroscopic behaviour of ferroelectric materials. *Phil. Mag. B* **81,** 2021–2054 (2001).
10. de Gennes, P.-G. & Okumura, K. Phase transitions of nematic rubbers. *Europhys. Lett.* **63,** 76–82 (2003).
11. Bhattacharya, K. *Microstructure of Martensite: Why it Forms and How it Gives Rise to the Shape-Memory Effect* (Oxford Univ. Press, Oxford, 2003).
12. Ericksen, J. L. Weak martensitic transformations in Bravais lattices. *Arch. Ration. Mech. Anal.* **107,** 23–36 (1989).
13. Tolédano, P. & Dmitriev, V. *Reconstructive Phase Transitions* (World Scientific, Singapore, 1996).
14. Maki, T. & Tamura, I. in *Proc. Int. Conf. on Martensitic Transformations* 963–970 (The Japan Institute of Metals, Nara, 1986).
15. Barker, L. M. & Hollenbach, R. E. Shock wave study of the $\alpha \leftrightarrow \varepsilon$ phase transition in iron. *J. Appl. Phys.* **45,** 4872–4887 (1974).
16. Kadau, K., Germann, T. C., Lomdahl, P. S. & Holian, B. L. Microscopic view of structural phase transitions induced by shock waves. *Science* **296,** 1681–1684 (2002).
17. Liu, Y. *et al.* Thermomechanical behaviour of fcc ↔ hcp martensitic transformation in CoNi. *J. Alloys Compd.* (in the press).
18. Matsumoto, S., Sato, A. & Mori, T. Formation of h.c.p. and f.c.c. twins in an Fe-Mn-Cr-Si-Ni alloy. *Acta Metall. Mater.* **42,** 1207–1213 (1994).
19. Yang, J. H. & Wayman, C. M. On secondary variants formed at intersections of ε martensite variants. *Acta Metall. Mater.* **40,** 2011–2023 (1992).
20. Lee, H. H. *et al.* Orientational proliferation and successive twinning from thermoreversible hexagonal-body-centered cubic transitions. *Macromolecules* **35,** 785–794 (2002).
21. Otsuka, K. & Shimizu, K. On the crystallographic reversibility of martensitic transformations. *Scripta Met.* **11,** 757–760 (1977).
22. Schwarzenberger, R. L. E. Classification of crystal lattices. *Proc. Camb. Phil. Soc.* **72,** 325–349 (1972).
23. Pitteri, M. & Zanzotto, G. *Continuum Models for Phase Transitions and Twinning in Crystals* (Chapman & Hall/CRC, Boca Raton, 2002).
24. Ericksen, J. L. Some phase transitions in crystals. *Arch. Ration. Mech. Anal.* **73,** 99–124 (1980).
25. Pitteri, M. Reconciliation of local and global symmetries of crystals. *J. Elast.* **14,** 175–190 (1984).
26. Ball, J. M. & James, R. D. Proposed experimental tests of a theory of fine microstructure and the two-well problem. *Phil. Trans. R. Soc. Lond. A* **338,** 389–450 (1992).
27. Fonseca, I. Variational methods for elastic crystals. *Arch. Ration. Mech. Anal.* **97,** 189–220 (1987).
28. Hull, D. & Bacon, D. J. *Introduction to Dislocations* 3rd edn (Pergamon, Oxford, 1984).
29. Conti, S. & Zanzotto, G. A variational model for reconstructive phase transformations in crystals, and their relation to dislocations and plasticity. *Arch. Ration. Mech. Anal.* (in the press).
30. Hua, L. K. & Reiner, I. On the generators of the symplectic modular group. *Trans. Am. Math. Soc.* **65,** 415–426 (1949).

Acknowledgements This work was largely carried out when J.Z. held a position at the California Institute of Technology. The work of S.C. and J.Z. was partially supported by the Deutsche Forschungsgemeinschaft. G.Z. acknowledges the partial support of the Italian MIUR (CoFin Modelli Matematici per i Materiali). S.C. and G.Z. acknowledge the partial support of the IV Framework Programme of the EU. K.B. and J.Z. acknowledge the partial financial support of the US Air Force Office of Scientific Research and the US Office of Naval Research. All authors contributed equally to this work.

Competing interests statement The authors declare that they have no competing financial interests.

Correspondence and requests for materials should be addressed to K.B. (bhatta@caltech.edu).

Polar ocean stratification in a cold climate

Daniel M. Sigman[1], Samuel L. Jaccard[2] & Gerald H. Haug[3]

[1]*Department of Geosciences, Princeton University, Princeton, New Jersey 08544, USA*
[2]*Department of Earth Sciences, ETH, CH-8092 Zürich, Switzerland*
[3]*Geoforschungszentrum Potsdam, D-14473 Potsdam, Germany*

The low-latitude ocean is strongly stratified by the warmth of its surface water. As a result, the great volume of the deep ocean has easiest access to the atmosphere through the polar surface ocean. In the modern polar ocean during the winter, the vertical distribution of temperature promotes overturning, with colder water over warmer, while the salinity distribution typically promotes stratification, with fresher water over saltier. However, the sensitivity of seawater density to temperature is reduced as temperature approaches the freezing point, with potential consequences for global ocean circulation under cold climates[1,2]. Here we present deep-sea records of biogenic opal accumulation and sedimentary nitrogen isotopic composition from the Subarctic North Pacific Ocean and the Southern Ocean. These records indicate that vertical stratification increased in both northern and southern high latitudes 2.7 million years ago, when Northern Hemisphere glaciation intensified in association with global cooling during the late Pliocene epoch. We propose that the cooling caused this increased stratification by weakening the role of temperature in polar ocean density structure so as to reduce its opposition to the stratifying effect of the vertical salinity distribution. The shift towards stratification in the polar ocean 2.7 million years ago may have increased the quantity of carbon dioxide trapped in the abyss, amplifying the global cooling.

The Subarctic Zone in the North Pacific Ocean and the Antarctic Zone in the Southern Ocean are both characterized by year-round availability of the 'major nutrients' nitrate and phosphate. Nutrient-rich deep water is brought to the surface by wind-driven upwelling and density-driven overturning. Limitation of algal growth by light[3] and iron[4] prevents complete consumption of the major nutrients. The Subarctic Pacific maintains a higher degree of nutrient utilization (and thus lower surface nutrient concentrations) than does the Antarctic[5]. There are two likely causes for this difference. First, the exchange between the surface and deep ocean is reduced in the Subarctic Pacific relative to the Antarctic. This is partially due to the stronger 'halocline', or vertical salinity gradient, in the Subarctic Pacific[6] (Fig. 1). Second, atmospheric deposition supplies more iron to the Subarctic Pacific than to the Antarctic, which should allow phytoplankton to consume a larger fraction of the upwelled nitrate and phosphate[4].

Despite the differences between these two polar ocean regions, the sediments underlying them show a similar change during the global cooling from the relatively warm mid-Pliocene to the late Pliocene, when the Earth descended into the Pleistocene cycle of ice ages. In both of these regions, upon the intensification of major Northern Hemisphere glaciation 2.7 million years ago (2.7 Myr), the accumulation of biogenic opal decreased abruptly, just when the sedimentary evidence indicates an increase in Northern Hemisphere sea ice and icebergs[7,8] (Figs 1 and 2; additional references in Fig. 1 legend). In the Antarctic, this shift has been interpreted as the result of increased sea ice cover shortening the productive season of diatoms[8,9], whereas the Subarctic Pacific change has been explained as the onset of permanent stratification reducing the nutrient supply to the surface[7]. Yet the similarity in the structure and timing of these changes invites a single explanation